Available online at www.sciencedirect.com
SCIENCE DIRECT®
Journal of Crystal Growth 265 (2004) 250–259
JOURNAL OF CRYSTAL GROWTH
www.elsevier.com/locate/jcrysgro

One-pot synthesis and characterization of high-quality CdSe/ZnX (X = S, Se) nanocrystals via the CdO precursor

Guo-Wei Huang, Chun-Yen Chen, Kun-Chan Wu, Moawia O. Ahmed, Pi-Tai Chou*

Department of Chemistry, The National Taiwan University, Taipei 106, Taiwan, ROC

Received 25 April 2003; accepted 30 January 2004
Communicated by R. James

Abstract

We report on the synthesis of CdSe/ZnX (X = S, Se) core/shell quantum dots from the CdO precursor through a convenient, one-pot approach. The defocusing stage (i.e., Ostwald Ripening) can be finely controlled to prepare nearly monodispersive core/shell quantum dots. The resulting particles have been characterized by their corresponding optical properties, energy dispersive spectroscopy, X-ray photoelectron spectroscopy, transmission electron microscopy and powder XRD. This method is highly reproducible, and quantum efficiencies as high as 0.7 can be achieved.

PACS: 81.05.Dz; 79.60.Jv; 81.65.Rv; 81.10.Dn

Keywords: A1. Low dimensional structures; B1. Nanomaterials; B2. Semiconducting II–VI materials

1. Introduction

Due to their remarkable size-dependent photophysical properties and versatility toward chemical modification, semiconductor nanoparticles have received considerable attention (for selective examples, see Ref. [1]). Semiconductor nanoparticles such as cadmium chalcogenides with high luminescence yield, monodispersity, uniform size and shape have played an active role in biological labeling reagents (for recent representative applications, see Ref. [2]). Among numerous applications, the core-shell types of quantum dots have been proven to serve as a better probe than the bare core ones owing to their higher-emission quantum efficiency (quantum confinement) and thermal stability (protective surface), in particular, when subject to subsequent multiple-step chemical modification [3–7].

The use of dimethyl cadmium $Cd(CH_3)_2$ as a precursor in the process for the synthesis of high-quality cadmium chalcogenides has been well documented [8,9]. Unfortunately, the high toxicity and pyrophoric liability limit its availability in

*Corresponding author. Tel.: +886-2-23630231x3988; fax: +886-2-23695208.
E-mail address: chop@ntu.edu.tw (P.-T. Chou).

0022-0248/$ - see front matter
doi:10.1016/j.jcrysgro.2004.01.064

many places. Alternatively, CdO has recently been reported to be an ideal precursor toward synthesizing core Cd chalcogenide nanocrystals [5,10,11]. Its lower toxicity and good thermal stability make the synthetic route to Cd chalcogenides quantum dots feasible without restrictions on equipment and on severe conditions. Very recently, based on the CdO precursor Reiss et al. [5] reported a new synthetic route for the core/shell CdSe/ZnSe nanoparticles incorporating preparation, separation and purification of core material (CdSe), followed by a second-step shell (ZnSe) deposition.

In the course of developing chemically modified nanoparticles toward biological applications, on the premise of safety and available resources, we have made attempts to prepare CdSe/ZnX nanocrystals via the CdO precursor. To our experience, although the two-step approach is salient, a successful CdSe/ZnSe preparation from CdO in terms of good homogeneity in size distribution and luminescence efficiency greatly relies on the purity of core CdSe prior to the shell deposition [5]. Furthermore, the second-step core/shell synthesis involves a subtle mixing procedure between core and reagents for the shell, which inevitably requires extensive work. These concerns have motivated us to seek an alternative modification, aiming at simplicity in methodology with high particle quality being preserved. On the basis of one-pot reaction, we herein report a simple, reproducible synthetic protocol for preparing high-quality CdSe/ZnX core/shell nanoparticles.

The scheme for the one-pot synthesis of CdSe/ZnX quantum dots incorporates CdO in a coordinate mixture consisting of HDA (hexadecylamine), TOPO (tri-*n*-octylphosphine oxide) and TBP (tri-*n*-butylphosphine). HDA was used as the capping agent as well as the solvent system for the growth of CdSe and CdSe/ZnX nanocrystals, which also facilitates the focusing of the particle size, resulting in a much smaller size distribution [5,7]. These, in combination with fine control of the stoichiometry among reactants, led us to successfully prepare wavelength (i.e., size)-tunable CdSe/ZnX quantum dots as described below.

2. Experiments

2.1. Chemicals

TOPO (tech. grade 90%), TBP (tech. grade 98%) and HDA (90%) were purchased from Aldrich, SHOWA and TCI, respectively. In another approach, high-purity TOPO (99%, Aldrich) was also applied for a comparative study. CdO (99.99%), selenium (Se) powder 200 mesh (>99.5%) and sulfur (S) powder (99.5%) were obtained from Strem, ACROS and Alfa Aesar, respectively. Dimethylzinc ($Zn(CH_3)_2$, 2 M solution in toluene) and hexamethyldisilathiane ($(TMS)_2S$) were acquired from Aldrich. Zinc stearate was purchased from Riedel-deHaën. All reagents were used as received.

2.1.1. Method 1

Due to great concerns in the tunability of semiconductor nanocrystals, we first described a one-pot, tunable-size CdSe/ZnX synthesis. In this reaction scheme a mixture of CdO (0.04 g), HDA (5.67 g) and TOPO (5.67 g) was heated up to ~340°C under Ar flow on a Schlenk line. After the formation of a CdO–HDA complex, as indicated by the solution turning from reddish color to colorless, the system was allowed to cool to 260°C. As the temperature stabilized at 260°C for around 3–5 h, Se/TBP (0.03 g in 6 ml TBP) was quickly injected (<2 s) into the hot CdO/HDA/TOPO solution to proceed with the nucleation and the growth of CdSe nanocrystals. Due to the introduction of large amounts of TBP, the system temperature was further decreased to 230°C within ~30 s. Subsequently, the Zn/X/TBP shell stock solution was injected precisely to the core solution via the syringe pump at a rate of as slow as 0.1–0.15 ml/min, while the temperature remained at 230°C, so that the growth of CdSe/ZnX quantum dots could be extracted during the reaction. The injection of shell stock solution was divided into five portions at ~20 s intervals to minimize the nucleation of shell particles [3]. Upon injecting all the Zn/X/TBP shell stock solution, the reaction mixture was allowed to cool and stir at 110°C for a period of 1–2 h. The final molar ratio

between Cd/Se (core) and Zn/X (shell) was kept constant, typically ~1:4.

Zn/X/TBP shell stock solution was prepared with two types of precursors. For the first approach, a pyrophoric precursor was used by dissolving $Zn(CH_3)_2$ (~125 μl) and $(TMS)_2S$ (~130 μl) in TBP (5.3 ml) at room temperature. In other approach, zinc stearate was used as a shell precursor to suit safety and green chemistry, which has been proven to be appropriate for the growth of ZnSe shells on the CdSe nanocrystals [5], albeit there is a large lattice mismatch between CdSe and ZnSe [6]. In this study, zinc stearate (0.76 g) and sulfur powder (0.02 g) in TBP (5.3 ml) were used and heated to ~110°C for 30 min. The shell stock solution prepared was then allowed to cool to room temperature for the subsequent core/shell synthesis.

For the above-described core/shell formation, the precursor concentrations were largely diluted by TBP and HDA, resulting in a significant reduction of the particle growth rate. The resulting nanocrystals with selective diameters/thickness could thus be extracted at different aging times. Consequently, the tunability of CdSe/ZnS nanocrystals was largely elevated.

2.1.2. Method 2

We also attempted to scale up the one-pot CdSe/ZnS production, aiming at unique-size distribution, while the emission wavelength needs no specification as long as the size distribution is insignificant with respect to the reaction time. To achieve this goal method 1 was modified by optimizing the reaction parameters such as Cd/Se ratio, TBP/HDA concentrations, etc. (vide infra). For a typical approach, CdO (0.04 g), TOPO (5.67 g) and HDA (2.83 g) were first loaded in a 50 ml three-neck flask and heated to ~340°C under argon flow on a Schlenk line. After forming a CdO–HDA complex, the system was then cooled down to ~260°C, followed by a rapid (<2 s) injection of the Se/TBP stock solution (0.013 g Se in 1 ml TBP). After this process, the temperature was allowed to cool to 230°C within a long period of 20 min, which was then suitable to passivate the ZnX shell by the addition of Zn/X/TBP. The Zn/X/TBP shell stock solution was similarly prepared from the aforementioned methods. The injection of shell stock solution was also divided into five portions at ~20 s intervals at a rate of as slow as 0.05–0.15 ml/min to avoid small size particles and/or alloy formation. Upon injecting all the Zn/X/TBP shell stock solution, the reaction mixture was then incubated at 110°C for a period of 1–2 h to obtain CdSe/ZnX particles with an emission maximized typically at ~635 nm.

For the above-described methods, purification was performed by adding anhydrous methanol to precipitate the resulted nanocrystals, which were then accumulated by centrifuging. This precipitation/centrifugation process was repeated several times to further remove unreacted residues. A slight decrease in the quantum efficiency was observed during the purification process, and could be regained by adding an adequate amount of TBP in each interval of centrifugation [12b]. The resulting nanocrystals were redispersed in anhydrous toluene for further characterization.

Further attempts to tune the growth rate of CdSe/ZnS nanocrystals were made by varying temperatures from [260°C (Se/TBP); 230°C (shell)] to [230°C; 180°C]. The lower nucleation/growth temperature leads to the large reduction of the growth rate, so that particles with emission maxima between 560 and 600 nm could be obtained during a long separated period of ~1 h. The vastly extended aging time at lower temperatures provides great potential in synthesizing wide-tunable-range core/shell nanoparticles for future applications in multiple bio-labeling or LEDs. Unfortunately, the resulting nanocrystals revealed a small fraction of dual emission, possibly due to the alloy formation (vide infra).

3. Results and discussion

3.1. Reaction parameters

Fig. 1A depicts the absorption and emission spectra of various sizes of CdSe/ZnS quantum dots prepared according to the tunable wavelength, one-pot reaction scheme (i.e., method 1). In each prepared sample the size distribution is rather small, as indicated by their narrow emission

FWHM of ~30 nm as well as uniformity in the excited-state relaxation dynamics ($\tau_f \sim 20-25$ ns, see Table 1). Direct evidence of size distribution was given by the results of the transmission electron microscopy (TEM) image. For instance, the TEM image of the batch extracted at $\tau_f \sim 600$ nm revealed a fairly homogeneous size distribution of 5.5 ± 0.6 nm (see Fig. 2). High luminescence efficiency was observed in all the different sizes of quantum dots with quantum yields measured to be in the range of 0.4–0.7 (see Table 1). As shown in Fig. 1B, based on method 2, nearly time-independent, unique-size CdSe/ZnS nanocrystals were obtained throughout the reaction with a systematic emission maximized at ~635 nm. Using pyrophoric precursors, the quantum efficiency of the resulting CdSe/ZnS nanocrystals would consistently exceed 0.5, while it was slightly lower (0.3–0.5) by using the zinc stearate precursor, possibly due to its lower reactivity during the one-pot reaction.

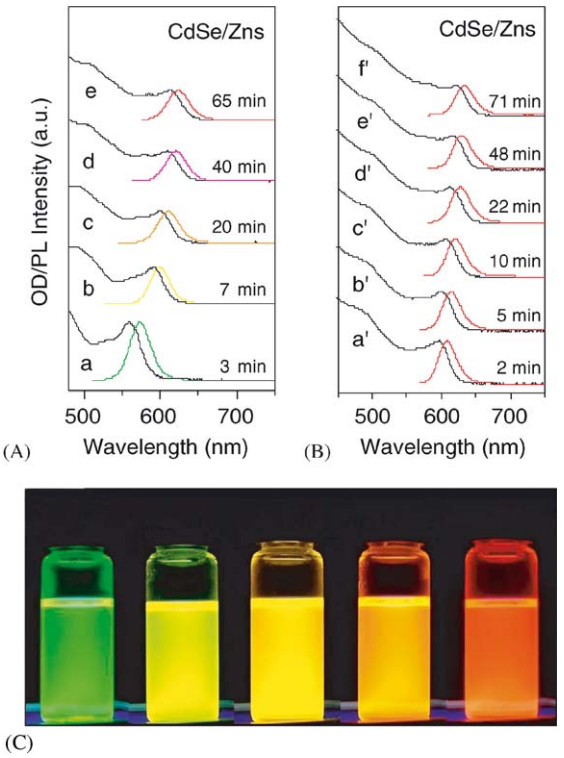

Fig. 1. Absorption and emission spectra of CdSe in toluene prepared from (A) method 1 and (B) method 2 (see text for the detailed description). The time scale for (A) and (B) is counted from the addition of Se/TBP (C) Authentic emission color of different shell thickness CdSe/ZnS nonocrystals acquired by a hand-held UV lamp with 366 nm excitation.

The initial Cd/Se molar ratio and precursor concentrations turn out to be key factors for obtaining size variable core/shell versus fixed-size nanocrystals within one-pot reaction. In this study, under optimized experimental conditions the initial Cd/Se ratio varied from ~0.7 in method 1 to ~2.0 in method 2, indicating the shift of the reaction parameters from a Se-rich to Cd-rich condition. Because the one-pot reaction scheme incorporates simultaneous growth of core and shell, the possibility of alloy formation has been carefully examined. Largely increasing the Cd/Se ratio caused adverse effects in method 1. For example, if we applied a Cd/Se ratio of >2.0, a minor, broad emission peak centered at ~500 nm

Table 1
Photophysics of various batches of quantum dots synthesized from this study

	Method 1(tunable size)				Method 2(unique size)		
Core/shell type[a]	$CdSe/ZnS^p$				$CdSe/ZnS^p$	$CdSe/ZnSe^z$	$CdSe/ZnS^z$
Compound[b]	a	b	c	d	f′	f_1	f_2
PL (λ_{max})	560	574	598	622	635	630	632
PL QY (%)[c]	46.2	51.3	67.3	65.1	52.8	48.5	49.7
τ_f (ns)	18.1(80[d])	20.3(85)	23.1(81)	21.2(91)	17.2(88)	20.1(80)	19.9(86)

[a] Superscripts p, z denote pyrophoric-, zinc sterate-related precursors, respectively.
[b] Compounds listed here correspond to Fig. 1; f_1,f_2, not shown in Fig. 1 correspond to the last batch (−70 min) of $CdSe/ZnSe^z$, $CdSe/ZnS^z$ nonocrystals, respectively.
[c] Reference for the quantum yield measurement is Rhodamine 6G.
[d] % of the major decay component.

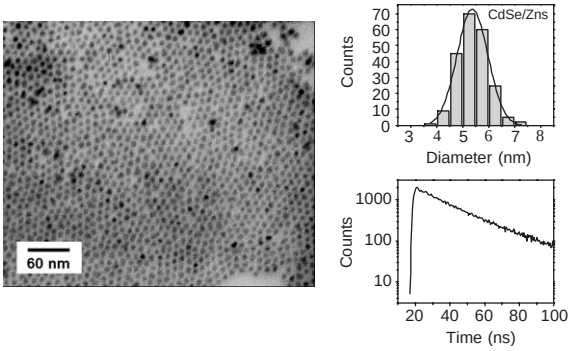

Fig. 2. TEM micrograph of CdSe/ZnS nanocrystals prepared by the tunable-size method (left), size distribution (upper right) and relaxation dynamics of compound c depicted in Fig. 1.

was observed, indicating a possible formation of $Cd_xZn_{1-x}S$ alloy (vide infra). In this study, it was found that the alloy formation could be avoided by reducing the Cd/Se ratio to <0.7 in method 1. On the other hand, due to the extended aging time for core growth prior to the shell addition in method 2, the possibility of alloy formation is considered small. Moreover, the higher Cd/Se ratio has been proven to have advantage in focusing the size distribution for hours before defocusing occurs [12a]. Consequently, the Cd-rich condition is suitable in method 2. Detailed characterizations of the core/shell formation are elaborated in Section 3.2.

The large increase of surfactants in method 1 dilutes precursor concentrations and consequently slows down the growth rate of core particles, so that the reaction time span is sufficiently long enough to deposit shell reagents at various core sizes. On one hand, as the precursor concentration is decreased, a large distribution of particle size is expected according to the Ostwald-Ripening defocusing mechanim [12], which explains that as the precursor concentrations decrease, the critical size of particles increases. As a result, the growth of smaller particles during the reaction may serve as nutrients for the larger ones, resulting in an increase in particle size as well as size distribution. On the other hand, it has been well documented that an increase of HDA leads to a reduction of size distribution, of which the phenomenon is analogous to a refocusing process [5,7]. The interplay between these two opposite effects can be compensated for by optimizing HDA/TBP concentrations, giving rise to decent particle-size tunablity with small size distribution as described in this study. In comparison, the time-independent, unique-size distribution obtained in method 2 can be qualitatively rationalized by the use of sufficiently low surfactant concentrations. Since surfactants act as capping agents as well as solvents, the precursor concentrations increase accordingly and the growth rate of the core is largely accelerated, eventually reaching a saturation of the particle size in a very short period. This synthetic protocol is particularly useful when a quick, large-scale synthesis of CdSe/ZnS nanocrystals is required without special consideration of the emission peak frequency.

One reaction parameter which deserves to be further discussed is the technical grade TOPO of 90% purity applied in our synthetic scheme. One might consider the impurity existing in TOPO, which mainly consists of octylphosphonic acid, may interfere with the CdO complex formation. To examine such a possibility, we performed control experiments by comparing HDA/TBP and TOPO (tech.-grade)/TBP solvent systems in synthesizing CdSe nanoparticles. In the HDA/TBP system, a color evolution from reddish to colorless was observed during the elevation of temperature. In contrast, for the CdO–TOPO mixture the reddish color remained unchanged for more than 4 h at 340°C. The results clearly indicate that the complex formation for CdO is mainly assisted by HDA. Further support was given by the synthesis of CdSe nanoparticles using high-purity TOPO (99%) in the HDA/TOPO system. Under the same one-pot reaction condition, we obtained the corresponding nanoparticles with optical properties similar to that synthesized by the tech.-grade TOPO.

3.2. Products characterization

Various techniques/spectroscopy were exploited to characterize the above-prepared nanocrystals. As shown in Fig. 3a and b, the elemental analysis based on the energy dispersive spectroscopy (EDX) offered an unambiguous evidence for the

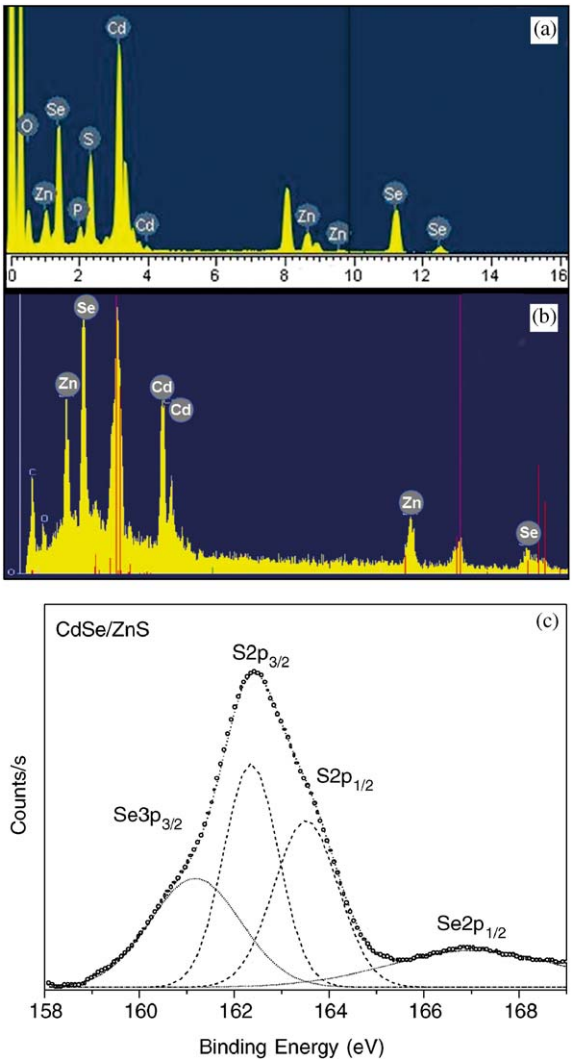

Fig. 3. EDX characterization of (a) CdSe/ZnS and (b) CdSe/ZnSe nanocrystals prepared by the one-pot reaction described in the text. (c) XPS characterization of CdSe/ZnS core/shell nanoparticles. The experimental data of CdSe/ZnS is fitted by four Gaussian peaks representing a S2p (dashed) and Se3p (dotted) contribution.

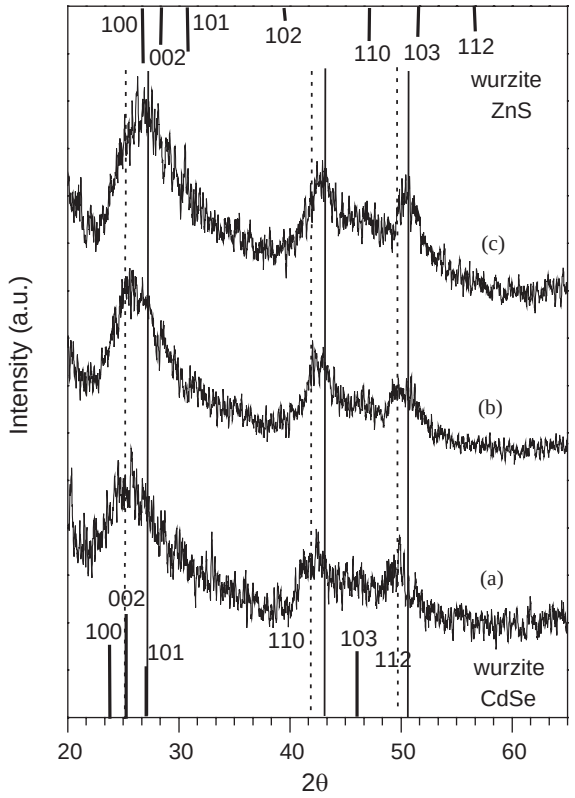

Fig. 4. Series X-ray powder diffraction patterns of (a) core CdSe nanocrystals with diameter ~4.6 nm, (b) core/shell CdSe/ZnS overcoated with ~1.5 ZnS ML and (c) ~3.6 ML ZnS-overcoated CdSe/ZnS nanoparticles. The solid vertical lines represent peak positions for sample (c, Fig. 4); the dotted lines represent pure wurzite CdSe crystal patterns. An evolution of peak shifting to higher 2θ value is detected upon shell passivation. The patterns for wurzite ZnS and CdSe are shown for comparison at the top and bottom insets, respectively.

presence of Cd/Se, Zn/S (or Zn/Se) components. Furthermore, X-ray photoelectron spectroscopy (XPS) signals collected on core/shell CdSe/ZnS nanocrystals also clearly indicated the co-existence of S and Se in the core/shell structure by the appearance of the characteristic peaks such as $S2p_{1/2}$, $S2p_{3/2}$, $Se3p_{1/2}$, and $Se3p_{3/2}$ (see Fig. 3c).

We have also performed X-ray powder diffraction to examine the patterns of a series of CdSe and CdSe/ZnS nanoparticles. As shown in Fig. 4, upon ZnS encapsulation the diffraction patterns shift gradually to high reflection angles. The result is a similar trend as that reported by Dabbousi et al. [4e] on the growth of core/shell nanoparticles. Note recent studies on ternary $Cd_xZn_{1-x}S$ nanocrystals also indicated that by decreasing the Cd/Zn molar ratio in alloy the diffraction patterns gradually, 2θ shifted to higher values. However, for a homogeneous alloy one would expect a narrowing XRD peak width upon increasing the

particle size [13]. In contrast, a slight peak broadening was observed upon the shell addition (see Fig. 4), supporting the core/shell formation in the one-pot reaction scheme. More characterizations of the core/shell composition are elaborated as follows.

For nanocrystals with alloy compositions, one would expect a blue shift of the first exciton peak upon increasing the dopant concentration [13]. Furthermore, for the $Cd_xZn_{1-x}S$ alloy a characteristic broad emission band at the region of $\sim$480–550 nm is normally expected [14]. In our tunable-size reaction scheme, the systematic red shift of the absorption/emission spectra upon the encapsulation of ZnS (or ZnSe), in combination with the absence of $<$550 nm emission, negates the possibility of alloy formation. Nevertheless, as was mentioned in the previous section, when the initial Cd/Se ratio in method 1 was increased to as high as $>$2.0, dual emission appeared, in which the minor one maximized at $\sim$500 nm may partially be attributed to the formation of $Cd_xZn_{1-x}S$ composites.

Theoretically, comparing the core only with the same diameter, spectral red shifts in core/shell nanoparticles are mainly due to the extent of excited electron wavefunction into the shell region, of which the degree of shifting depends on the band-offset between core and shell. However, with a large band-offset, the probability of excited electrons populated at the shell region is considered small. Accordingly, due to their large band-offset a small spectral red shift is predicted upon CdSe/ZnX formation, which apparently cannot rationalize the $\sim$60 nm tunability throughout the one-pot reaction. The results clearly indicate that HDA/TBP simultaneously controlled the growth of core particles and the shell encapsulation. The combination of these two factors plays a key role in fine-tuning the wavelength (i.e., size) and/or shell thickness.

Finally, control experiments have been performed based on the tunable-size synthetic protocol to compare the properties between core only and core/shell nanoparticles. Under identical experimental conditions, i.e., the same Cd/Se ratio, surfactant concentrations, aging times, etc., the emission spectrum in each batch of the core/shell

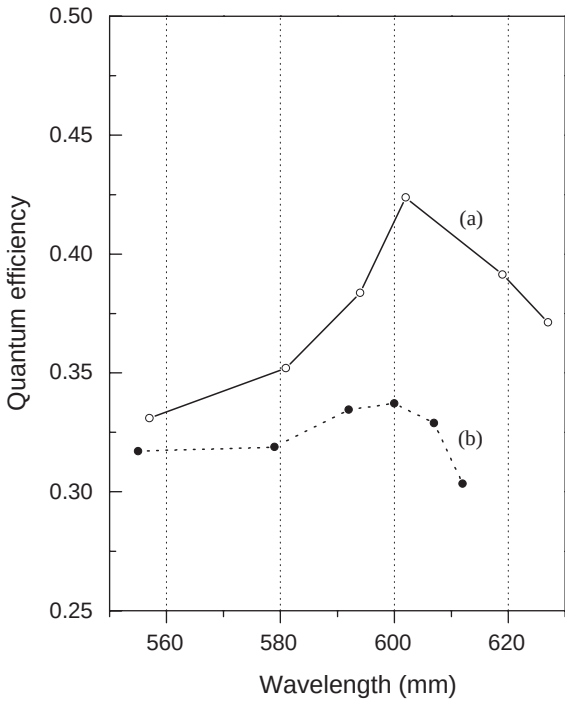

Fig. 5. Control experiments performed on method 1 (tunable-size) with 6 different aging times (12 aliquots) are compared. Line (a) shows the evolution and properties of core/shell formation, while (b) depicts the properties of core only during the growth process. Note: the shell stock solution applied here for core/shell formation is zinc stearate/sulfur/TBP.

formation is red shifted with respect to that of the core-only one (see Fig. 5). The result reveals that further increase of the core/shell particle size is mainly attributed to the shell passivation. Further photophysical supports were rendered by the enhancement of the quantum efficiency on the core/shell structure in comparison to the core only particles synthesized via the same approach. The results clearly reveal the existence of improved passivation as well as the protective-type structure generated on the resulted core/shell particles. The shell passivation was also confirmed by comparing the resulting particle sizes from TEM micrographs, in which within an identical aging time the average size calculated for core/shell particles is larger than that of the core only. Taking the thickness of ZnS monolayer (ML) to be 0.31 nm [4e], the number of ZnS MLs overcoated on CdSe of batches 4 and 6

in Fig. 5 was estimated to be ~1.5 and 3.6 ML, respectively.

The above experiments/observations provide unambiguous evidence for the one-pot core/shell nanoparticles formation. One of our future aims is to develop chemically modified nanoparticles toward the biochemical application. To achieve this goal, we herein also demonstrated the feasibility of water-soluble quantum dots preparation based on the synthesized core/shell nanoparticles. In this preliminary study, a water-soluble 2-(12-Mecaptododecyloxy) methyl-15-crown ether capped CdSe/ZnS core-shell was prepared by a standard surfactant desorption/ligand exchange technique [2f,15], in which 2-(12-mecaptododecyloxy) methy l-15-crown ether was synthesized by the alkylation of 2-(hydroxymethyl)-15-crown-5 ether with dibromododecane, followed by the replacement of the bromo- by thio-group in the presence of thiourea [16]. The resulted two

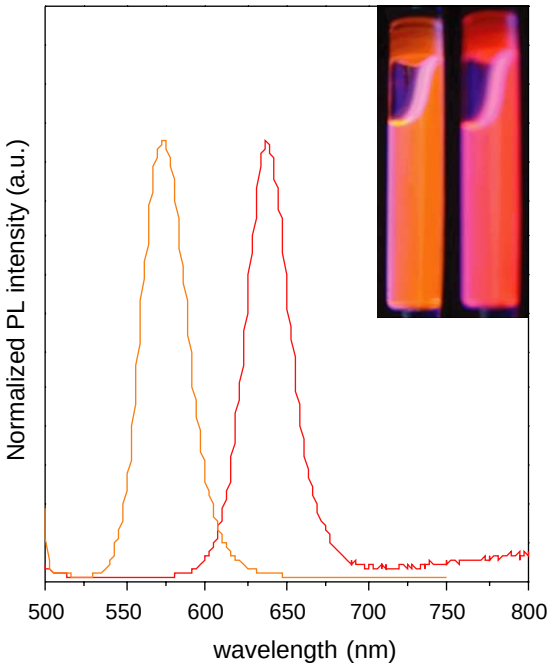

Fig. 6. Emission spectra of two different sized 2-(12-mecaptododecyloxy) methyl-15-crown ether capped CdSe/ZnS nanoparticles in aqueous solution (pH ~9). Inset shows the authentic emission color of these two water-soluble CdSe/ZnS quantum dots acquired by a hand-held UV lamp with 366 nm excitation.

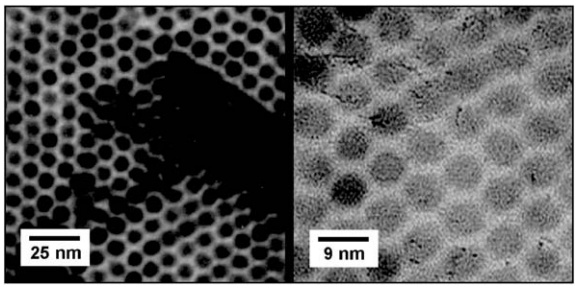

Fig. 7. TEM image of core CdSe nanoparticles prepared from the CdO/HDA reaction system.

different size QDs show naked eye detectable emission light with fluorescent quantum efficiency (Q.Y.) of ~0.1, possessing a ~30 nm bandwidth maximized at 580 and 636 nm, respectively (see Fig. 6). In a comparative study, the same synthetic protocol was applied on the core-only CdSe. The fluorescence of the resulting water-soluble CdSe was completely quenched in aqueous solution, possibly due to the lack of shell protection.

3.3. Comparing current methods

Finally, comparisons have been made here regarding other synthetic approaches. Using CdO as a precursor, the synthesis of core Cd chalcogenides has been reported by exploiting a combination of tetradecylphosphonic acid (TDPA)/TOPO/tri-*n*-octylphosphine (TOP) ligands [10]. From the economic viewpoint, HDA used in this study is much less expensive than TDPA. Although TDPA exhibits higher reactivity than HDA in complexing CdO, the aging time for the complex formation can still be fully accomplished within 1 h using HDA. As shown in Fig. 7, using CdO as a precursor, in combination with the HDA ligand, we have also successfully prepared high-quality core CdSe with a uniform size distribution.[1] Obviously, this advantage may play a key

[1] Synthesis of high-quality CdSe nanocrystals: 0.02 g of CdO, 2.8 g of TOPO and 1.4 g of HDA were loaded into a three-neck flask. The mixture was heated to 330°C under argon flow to form the colorless complex. As the temperature stabilized at 260°C, the Se/TBP stock solution (0.016 g of Se/1 ml TBP) was introduced and further growth of crystals was proceeded at 250°C.

role for future scaled-up production. As described in an earlier section, Reiss et al. [5] have developed a method incorporating safer agents into the core/shell preparation, yet TDPA and a nontrivial, two-step synthetic process are involved. In addition, the shell materials (zinc stearate/Se/toluene) applied in Reiss et al.'s work were found inappropriate in our one-pot reaction scheme, although the actual mechanism remains unsolved at this stage. To make a successful one-pot reaction, shell composites were modified by substituting toluene to TBP. Furthermore, we also succeeded in synthesizing CdSe/ZnS nanocrystals simply by replacing Se with sulfur powder, indicating the versatility and simplicity of the one-pot reaction scheme.

Using $Cd(CH_3)_2$ as a precursor encapsulated by HDA ligand, Talapin et al. [7] reported on the preparation of CdSe/ZnS nanocrystals based on a two-step synthesis incorporating preparation and separation of core CdSe, followed by the second reaction involving pyrophoric Zn/S stock solution. Finally, via the $Cd(CH_3)_2$ precursor Hines and Guyot-Sionnest have reported on the one-pot synthesis of CdSe/ZnS nanocrystals in the TOP/TOPO system [3]. Under their reaction circumstances described, we have attempted to synthesize naocrystals via CdO precursors but unfortunately failed. Interestingly, in Hines et al.'s work, the spectral shift in terms of peak frequencies is small between core and core/shell, and could be explained by a decrease of the kinetic energy of the excited electron wavefunction upon spreading wavefunctions into the shell. In comparison, a wide range of tunability of ~ 60 nm was consistently observed in our one-pot synthetic scheme. Similar phenomena were also observed in Talapin et al.'s work, indicating that the encapsulation of ZnS shell is accompanied by the growth of CdSe in HDA-related systems.

4. Conclusions

In conclusion, we have prepared CdSe/ZnX (X = S, Se) quantum dots from the CdO precursor through a convenient, one-pot approach to maintain simplicity and green chemistry [17]. Various characterization experiments provide unambiguous evidence for the core/shell nanoparticles formation. The feasibility of synthesizing tunable-size core/shell quantum dots may be considered an advantage, although the growing mechanism seems relatively complicated, as it may simultaneously incorporate the growth of core and the shell passivation. Nevertheless, the synthetic scheme described here optimized and finely controlled the defocusing stage, so that high-quality core/shell CdSe/ZnX quantum dots can be prepared in a one-pot synthesis. Based on the resulting CdSe/ZnS nanocrystals, we have succeeded in preparing various sizes 2-(12-mecaptododecyloxy) methyl-15-crown ether capped CdSe/ZnS quantum dots with emission yield up to ~ 0.1. Focus on the corresponding biochemical applications will be published elsewhere.

Acknowledgements

We thank Professor Peter Reiss for providing useful suggestions. We also thank Ching-Yen Lin and Chih-Yuan Tang in Instrumentation Center, National Taiwan University for assistance with the TEM measurements. This work is financially supported by National Science Council of the Republic of China.

References

[1] (a) Al.L. Efros, A.L. Efros, Sov. Phys. Phys. Semicond. 16 (1982) 772;
(b) L.E. Brus, J. Chem. Phys. 80 (1984) 4403;
(c) M.G. Bawendi, M.L. Steigerwald, L.E. Brus, Annu. Rev. Phys. Chem. 41 (1990) 477;
(d) L.E. Brus, Appl. Phys. A 53 (1991) 465;
(e) Y. Wang, N. Herron, J. Phys. Chem. 95 (1991) 525;
(f) J.R. Heath, Science 258 (1992) 1131;
(g) A.P. Alivisatos, Science 271 (1996) 933;
(h) S.V. Gaponenko, Optical Properties of Semiconductor Quantum Dots, Springer, Berlin, 1996;
(i) M. Nirmal, L.E. Brus, Acc. Chem. Res. 32 (1999) 407;
(j) Al.L. Efros, M. Rosen, Annu. Rev. Mater. Sci. 30 (2000) 475.
[2] (a) M. Bruchez Jr., M. Moronne, P. Gin, S. Weiss, A.P. Alivisatos, Science 281 (1998) 2013;
(b) W.C.W. Chan, S. Nie, Science 281 (1998) 2016;

(c) H. Mattoussi, J.M. Mauro, E.R. Goldman, G.P. Anderson, V.C. Sundar, F.V. Mikulec, M.G. Bawendi, J. Am. Chem. Soc. 122 (2000) 12142;
(d) S.R. Whaley, D.S. English, E.L. Hu, P.F. Barbara, A.M. Belcher, Nature 405 (2000) 665;
(e) C.M. Niemeyer, Angew. Chem. Int. Ed. 40 (2001) 4128;
(f) S.J. Rosenthal, I. Tomlinson, E.M. Adkins, S. Schroeter, S. Adams, L. Swafford, J. McBride, Y. Wang, L.J. DeFelice, R.D. Blakely, J. Am. Chem. Soc. 124 (2002) 4586;
(g) W.C. Chan, D.J. Maxwell, X. Gao, R.E. Bailcy, M. Han, S. Nie, Curr. Opin. Biotechnol. 13 (2002) 40;
(h) M.E. Åkerman, W.C.W. Chan, P. Laakkonen, S.N. Bhatia, E. Ruoslahti, PNAS 99 (2002) 12617.
[3] M.A. Hines, P. Guyot-Sionnest, J. Phys. Chem. 100 (1996) 468.
[4] (a) L. Spanhel, M. Haase, H. Weller, A. Henglein, J. Am. Chem. Soc. 109 (1987) 5649;
(b) A.R. Kortan, R. Hull, R.L. Opila, M.G. Bawendi, M.L. Steigerwald, P.J. Carroll, L.E. Bruset, J. Am. Soc. Chem. 112 (1990) 1327;
(c) A. Mews, A.V. Eychmuller, M. Giersig, D. Schooss, H. Weller, J. Phys. Chem. 98 (1994) 934;
(d) M. Danek, K.F. Jensen, C.B. Murray, M.G. Bawendi, Appl. Phys. Lett. 65 (1994) 2795;
(e) B.O. Dabbousi, J. Rodroguez-Viejo, F.V. Mikulec, J.R. Heine, H. Mattoussi, R. Ober, K.F. Jensen, M. Bawendi, J. Phys. Chem. B 101 (1997) 9463;
(f) D. Gerion, F. Pinaud, S.C. Williams, W.J. Parak, D. Zanchet, S. Weiss, A.P. Alivisatos, J. Phys. Chem. B 105 (2001) 8861;
(g) M.A. Malik, P. O'Brien, N. Re vaprasadu, Chem. Mater. 14 (2002) 2004.
[5] P. Reiss, J. Bleuse, A. Pron, Nano Lett. 2 (2002) 781.
[6] (a) C.F. Hoener, K.A. Allen, A.J. Bard, A. Campion, M.A. Fox, T.E. Mallouk, S.E. Webber, J.M. White, J. Phys. Chem. 96 (1992) 3812;
(b) M. Danek, K.F. Jensen, C.B. Murray, M.G. Bawendi, Chem. Mater. 8 (1996) 173.
[7] D.V. Talapin, A.L. Rogach, A. Kornowski, M. Haase, H. Weller, Nano Lett. 1 (2001) 207.
[8] C.B. Murray, D.J. Norris, M.G. Bawendi, J. Am. Chem. Soc. 115 (1993) 8706.
[9] (a) C.B. Murray, C.R. Kagan, M.G. Bawendi, Annu. Rev. Mater. Sci. 30 (2000) 545;
(b) X. Peng, L. Manna, W. Yang, J. Wickham, E. Scher, A. Kadavanich, A.P. Alivistos, Nature 404 (2000) 59;
(c) C. de Mollo Donegá, S.G. Hickey, S.F. Wuister, D. Vanmaekelbergh, A. Meijerink, J. Phys. Chem. B 107 (2003) 489.
[10] Z.A. Peng, X. Peng, J. Am. Soc. Chem. 123 (2001) 183.
[11] L. Qu, X. Peng, J. Am. Chem. Soc. 124 (2002) 2049.
[12] (a) X. Peng, J. Wickham, A.P. Alivisatos, J. Am. Chem. Soc. 120 (1998) 5343;
(b) D.V. Talapin, A.L. Rogach, E.V. Shevchenko, A. Kornowski, M. Haase, H. Weller, J. Am. Chem. Soc. 124 (2002) 5782.
[13] X. Peng, M.C. Schlamp, A. Kadavanich, A.P. Alivisatos, J. Am. Chem. Soc. 119 (1997) 7019.
[14] (a) W. Wang, I. Germanenko, M.S. El-Shall, Chem. Mater. 14 (2002) 3028;
(b) S.M. Zhou, Y.S. Feng, L.D. Zhang, J. Crystal Growth 252 (2003) 1.
[15] S-Y. Lin, S-W. Liu, C-M. Lin, C-H. Chen, Anal. Chem. 74 (2002) 330.
[16] (a) S. Flink, B.A. Boukamp, A. v d Berg, F.C.J.M. v Veggel, D.N. Reinhoudt, J. Am. Chem. Soc. 120 (1998) 4652;
(b) S. Flink, F.C.J.M. v Veggel, D.N. Reinhoudt, J. Phys. Chem. B 103 (1999) 6515.
[17] (a) W. Leitner, Science 284 (1999) 1780;
(b) X. Peng, Chem. Eur. J. 8 (2002) 335.